

# Reductive Control in the Management of Redundant Actuation

Mkhinini Maher, Knani Jilani

**Abstract**—We present in this work the performances of a mobile omnidirectional robot through evaluating its management of the redundancy of actuation. Thus we come to the predictive control implemented.

The distribution of the wringer on the robot actions, through the inverse pseudo of Moore-Penrose, corresponds to a « geometric » distribution of efforts. We will show that the load on vehicle wheels would not be equi-distributed in terms of wheels configuration and of robot movement.

Thus, the threshold of sliding is not the same for the three wheels of the vehicle. We suggest exploiting the redundancy of actuation to reduce the risk of wheels sliding and to ameliorate, thereby, its accuracy of displacement. This kind of approach was the subject of study for the legged robots.

**Keywords**—Mobile robot, actuation, redundancy, omnidirectional, inverse pseudo Moore-Penrose, reductive control.

## I. INTRODUCTION

ON mobile robotics, few vehicles are kinematically redundant. The joint variables (angular velocities of rotation and wheels' orientation), are constrained by the relations of rolling without sliding in the contact point wheel/soil and the increase on wheels number doesn't increase the redundancy. Despite the fact that a big number of vehicles present a redundancy of actuation, it was compulsory to wait the late nineties for that feature to be valorized on the omnidirectional vehicles in particular.

## II. MANAGEMENT OF THE REDUNDANCY OF ACTUATION

### A. Opposite Dynamic Model

The opposite dynamic model of the vehicle provides the dynamic wringer in the center of the mark robot.

In the case of a robot possessing as many actuators as liberty degrees and out of singular configuration, the inversion of the jacobian is possible. In the other cases, the opposite generalized matrices allow obtaining a solution.

The Pseudo-Inverse of Moore-Penrose, practice to implement, doesn't benefit from the redundancy of actuation of the robot. It provides the solution of minimal Euclidean norm.

Other approaches, developed especially for the manipulator robots, allow the simultaneous accomplishment of the movement and of a secondary [6], [8], [9].

Mkhinini Maher is with Esprit-Tech: R&D department, the ESPRIT: School of Engineering and Technology Tunis, Tunisia (e-mail: maherrmkh@gmail.com).

Knani Jilani was with Laboratoire LARA, ENITBP 37, Le Belvédère 1002 Tunis, Tunisia (e-mail: Jilani.knani@enit.rnu.tn).

$$\begin{pmatrix} 1 & 1 & 1 \\ y_{r1}(\beta_1) & y_{r2}(\beta_2) & y_{r3}(\beta_3) \\ x_{r1}(\beta_1) & x_{r2}(\beta_2) & x_{r3}(\beta_3) \end{pmatrix} \cdot \begin{pmatrix} N_1 \\ N_2 \\ N_3 \end{pmatrix} = \begin{pmatrix} -M_{pl} \cdot g \\ h \cdot F_3 \\ h \cdot F_3 \end{pmatrix} \quad (1)$$

### B. Study of the Redundancy

The kinematic redundancy is expressed in the space of velocities. The redundancy of actuation is expressed in space of efforts.

A kinematically redundant robot can accomplish a task without using the totality of its joints. Practically, one or several of its joints, considered as secondary, could be blocked without harming the mobility of the terminal organ of the robot.

All robots' joints presenting a redundancy of actuation without being kinematically redundant are necessary in the completion of the task. Some joints could, however, move passively, i.e. driven by the forces transmitted by the other bodies or the ground.

### C. Redundancy of Actuation for the Kinematically Constrained Robots

For the robots with kinematic closed chain, the actuation speeds are linked by relations of kinematic constraints. This redundancy may appear on parallel robots [2], during the cooperation of many serial robots [3] or on some mobile robots when the number of chain actuators is upper than the number of the d.d.l. of the robot.

Although actuators' speeds are fully determined by the setpoint of operational speed, the redundancy of actuation allows the partition of the forces in order to produce the movement [11].

### D. Graphic Approach of Redundancy «Order 1»

The presence of solutions to the problem of partition is presented graphically in the case of a force to be spread over an eccentric two-wheeled fully motorized system.

Every couple of actuators ( $\tau_\alpha, \tau_\beta$ ) produces respectively the force  $f_1$  for the force  $f_2$ .

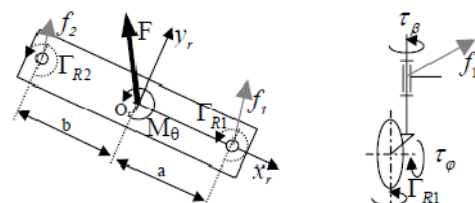


Fig. 1 Definition of the problem with two couples of actuators

The dynamic screw in the middle of the platform Or is composed of a force F and a moment M<sub>θ</sub>. We have a couple of actuators by a wheel to create the dynamic screw above.

The maximal force transmittable by each of the two wheels is noted respectively f<sub>1Max</sub> for wheel 1 and f<sub>2Max</sub> for wheel 2.

What is the combination of the forces f<sub>1</sub> and f<sub>2</sub> able to produce the desired dynamic screw?

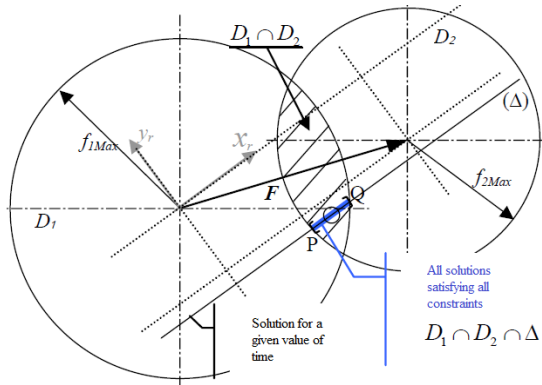


Fig. 2 Solutions to the problem of partition

The hatched area is the area of feasible solution from the point of view of the maximal. Every couple (f<sub>1</sub>, f<sub>2</sub>) of vectors which intersection belongs to this area checks the:

$$\begin{cases} F = f_1 + f_2 \\ |f_1| < f_{1Max} \\ |f_2| < f_{2Max} \end{cases} \quad (2)$$

The moment according to axis z<sub>r</sub> depends on the projections of f<sub>2</sub> on y<sub>r</sub>. Every couple of force f<sub>1</sub> and f<sub>2</sub> intersecting on a straight (Δ) parallel to x<sub>r</sub> corresponds to a constant moment.

F<sub>x</sub> et F<sub>y</sub> are the components of F in the reference mark, the system of equation to be solved has the following form:

$$\begin{pmatrix} F_x \\ F_y \\ M_z \end{pmatrix} = \begin{pmatrix} 1 & 1 & 0 & 0 \\ 0 & 0 & 1 & 1 \\ 0 & 0 & a & b \end{pmatrix} \cdot \begin{pmatrix} f_{1xr} \\ f_{2xr} \\ f_{1yr} \\ f_{2yr} \end{pmatrix} = J^T \cdot \begin{pmatrix} f_{1xr} \\ f_{2xr} \\ f_{1yr} \\ f_{2yr} \end{pmatrix}, M_z = M_z - \Gamma_{R1} - \Gamma_{R2} \quad (3)$$

where f<sub>1</sub> et f<sub>2</sub> are projected on x<sub>r</sub>, y<sub>r</sub>. the solutions of this system are written in the following way:

$$\begin{pmatrix} f_{1xr} \\ f_{2xr} \\ f_{1yr} \\ f_{2yr} \end{pmatrix} = (J^T)^+ \cdot \begin{pmatrix} F_x \\ F_y \\ M_z \end{pmatrix} + \lambda f \quad (4)$$

where f is an element of the nucleus of J<sup>T</sup>

$$f \in \text{Ker}(J^T) = \{x \in \mathbb{R}^4 / J^T x = 0\}$$

The elements of the nucleus of J<sup>T</sup> satisfy the equation f<sub>1xr</sub>=-f<sub>2xr</sub> which defines an orientation straight x<sub>r</sub>. The set of admissible solutions is given by the direction straight x<sub>r</sub> passing through the point defined by the solution of Moore-Penrose, and which the constraints, of nonsliding, are limited to the segment [PQ] (Fig. 3).

Le vector f allows the modification of the forces f<sub>1</sub> and f<sub>2</sub> in a way to produce the force and the moment M<sub>θ</sub> in the middle of the platform whilst ensuring the rolling of wheels without sliding.

#### E. Generalization to the Redundancy of Superior Order

If the robot has three couples of actuators to engender the plan dynamic screw, the solution is also obtained through the intersection, of the under-space verifying the constraints rolling without sliding and of the nucleus of the Jacobean transposed from the robot like in the mono-dimensional case; the constraints could be graphically visualized:

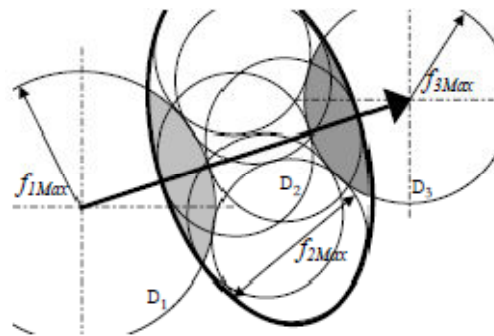


Fig. 3 Distribution over three motorized wheels

The ends of f<sub>1</sub>, f<sub>2</sub> et f<sub>3</sub> must be situated in the shaded areas.

In general case the nucleus is a variety of three dimensions.

Δ is the representative variety of the nucleus

D1 disk of f<sub>1Max</sub> radius

D2 disk of f<sub>2Max</sub> radius

D3 disk of f<sub>3Max</sub> radius

The eligible forces are such as the intersection of f<sub>1</sub> and f<sub>2</sub> situated on D<sub>1</sub>∩D<sub>2</sub>∩Δ and the intersection of f<sub>2</sub> and f<sub>3</sub> situated on D<sub>2</sub>∩D<sub>3</sub>∩Δ.

This set of system solutions could be written in the form of a sum of the given solution through the pseudo-inverse of Moore-Penrose and an element of the Jacobean matrix nucleus transposed from the robot [7].

$$\tau = J^{T+} F_{cart} + (I - J^{T+} J^T) \epsilon \quad (5)$$

where ε is the element of ℝ<sup>6</sup> and (I - J<sup>T+</sup>J<sup>T</sup>) is the projection operator on the nucleus of J<sup>T</sup>.

The couples of actuation depend then on the configuration of the robot.

#### F. Actuation Redundancy for the Mobile Robots with Directional Decentered Wheels

An entirely motorized decentered wheel is an actuator of two orthogonal degrees of liberty [6]. It allows the control of the two horizontal components of the transmitted force (Fig. 4).

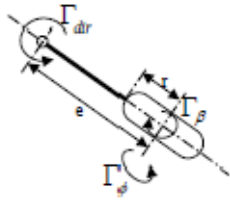


Fig. 4 Case of the fully actuated wheel

This wheel could always generate two degrees of orthogonal liberty, regardless its configuration compared with the movement.

### III. STUDY OF PARTICULAR MOVEMENTS

The kinematic model

$$\dot{q}_i = \begin{pmatrix} \frac{1}{r} & 0 \\ 0 & -\frac{1}{e} \end{pmatrix} \begin{pmatrix} \cos\beta_i & \sin\beta_i \frac{1}{r} (x_{Ai} \sin\beta_i - y_{Ai} \cos\beta_i) \\ \sin\beta_i & -\cos\beta_i \frac{1}{r} (e - x_{Ai} \cos\beta_i - y_{Ai} \sin\beta_i) \end{pmatrix} \cdot \eta_n \quad (6)$$

where  $\dot{q}_i = \begin{pmatrix} \dot{\phi}_i \\ \dot{\beta}_i \end{pmatrix}$  and  $\eta_n = R(\theta) \dot{\xi}_n$

$$\dot{\xi}_n = \begin{pmatrix} \dot{x} \\ \dot{y} \\ R\dot{\theta} \end{pmatrix} \text{ and } R(\theta) = \begin{pmatrix} \cos\theta & \sin\theta & 0 \\ -\sin\theta & \cos\theta & 0 \\ 0 & 0 & 1 \end{pmatrix}$$

In certain configurations of vehicle wheels, only one of the two actuators contributes in the movement.

Apply to the kinematic model of a wheel, defined by (5) the variable change:

$$V = \sqrt{(\dot{x} - y_A \dot{\theta})^2 + (\dot{y} - x_A \dot{\theta})^2} \quad (7)$$

where  $(\dot{x} - y_A \dot{\theta}) = v_x$  and  $(\dot{y} - x_A \dot{\theta}) = v_y$

The differential equation on  $\beta$ , subject to this change of variable, is written:

$$-\frac{e}{V} (\dot{\beta} + \dot{\theta}) = \sin\beta \frac{v_x}{V} - \cos\beta \frac{v_y}{V} \quad (8)$$

or:

$$-\frac{e}{V} (\dot{\beta} + \dot{\theta}) = \sin(\beta - \gamma) \text{ avec } \tan\gamma = \frac{v_y}{v_x}$$

While a pure movement of translation, the angular speed of orientation  $\dot{\theta}$  is zero.

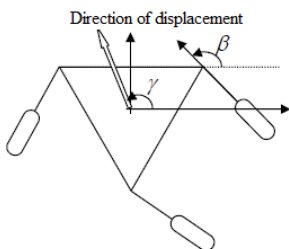


Fig. 5 Rectilinear movement

Suppose that the orientation of the wheel  $\beta$  is neighbor to the direction of the movement  $\gamma$ . Posing:

$$\beta = \gamma + \varepsilon$$

the previous equation is written

$$-\frac{e}{V} \dot{\varepsilon} = \sin(\gamma + \varepsilon) \frac{v_x}{V} - \cos(\gamma + \varepsilon) \frac{v_y}{V}$$

For small  $\varepsilon$ , we can write the linearized equation:

$$-\frac{e}{V} \dot{\varepsilon} = \sin(\gamma + \varepsilon \cos\gamma) \frac{v_x}{V} - \cos(\gamma + \varepsilon \sin\gamma) \frac{v_y}{V} - \frac{e}{V} \dot{\varepsilon} = \left( \frac{v_x}{V} \cos\gamma + \frac{v_y}{V} \sin\gamma \right) \varepsilon \quad (9)$$

$\varepsilon$  obeys then to the differential equation of first order:

$$\varepsilon + \frac{e}{V} \dot{\varepsilon} = 0 \quad (10)$$

$\varepsilon$  tends exponentially to 0, thus  $\beta$  tends exponentially to  $\gamma$ .

We can express the jacobian of the vehicle relative to this movement:

$$J_{R_t}^T = R(z_r, \gamma) J^T$$

We get:

$$J_{R_t}^T = \begin{pmatrix} \cos(\beta_1 - \gamma)/r & \cos(\beta_2 - \gamma)/r & \cos(\beta_3 - \gamma)/r & -\sin(\beta_1 - \gamma)/e & -\sin(\beta_2 - \gamma)/e & -\sin(\beta_3 - \gamma)/e \\ \sin(\beta_1 - \gamma)/r & \sin(\beta_2 - \gamma)/r & \sin(\beta_3 - \gamma)/r & \cos(\beta_1 - \gamma)/e & \cos(\beta_2 - \gamma)/e & \cos(\beta_3 - \gamma)/e \\ \Sigma 1/r & \Sigma 2/r & \Sigma 3/r & \Omega_{1/e} & \Omega_{2/e} & \Omega_{3/e} \end{pmatrix}$$

or

$$\begin{cases} \Sigma 1 = x_{Ai} \sin\beta_i - y_{Ai} \cos\beta_i \\ \Omega_1 = e - x_{Ai} \cos\beta_i - y_{Ai} \sin\beta_i \end{cases} \quad (11)$$

Once the three wheels are aligned, the representative matrices of the under spaces of traction and direction become:

$$J_{\phi}^T = \begin{pmatrix} 1/r & 1/r & 1/r \\ 0 & 0 & 0 \\ \Sigma 1/r & \Sigma 2/r & \Sigma 3/r \end{pmatrix} \quad (12)$$

$$J_{\beta}^T = \begin{pmatrix} 0 & 0 & 0 \\ 1/e & 1/e & 1/e \\ \Omega_{1/e} & \Omega_{2/e} & \Omega_{3/e} \end{pmatrix}$$

We draw two conclusions:

- \* The under spaces generated by the actuators of traction and direction are orthogonal and only the actuators of traction contribute in the rectilinear movements. They are orthogonal
- \* Each of the matrices contains three related vectors, the redundancy in relation with the movement is here of the order 2.

In the case of a rectilinear movement and once the wheels were aligned, only a one engine of traction is necessary for the movement. The two others are supernumerary. The same study could be carried out for other particular movements (Fig. 6); it leads to a similar result.

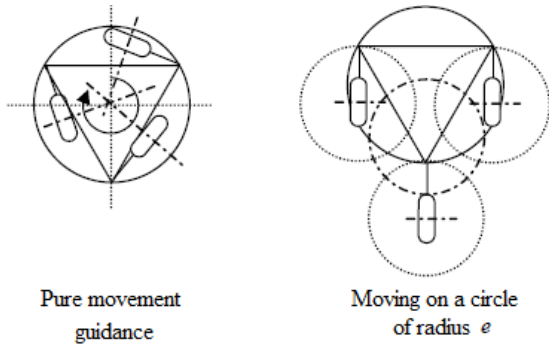


Fig. 6 Movements decoupling the actuators

According to Campion [4], an omnidirectional robot must be equipped at least of four engines in order to avoid any singular position. For example, if only the axes of traction are motorized and if the wheels are aligned, no lateral movement is then possible [1].

With four engines, an omnidirectional vehicle with decentered directional wheels presents- out of particular configurations- a redundancy of actuation. Beyond four engines, the redundancy of actuating becomes intrinsic.

In the case of the robot OMNI, equipped of three wheels fully motorized, the Jacobean matrix transposed of the vehicle is composed of six columns vectors. For a movement plan (2T + 1R), and out of particular configuration, the under spaces of traction and direction contributes together in the movement. The redundancy is in this case of « order 3 ». In the most unfavorable case of a movement decoupling the under spaces, it is still « of order 2 ». The robot OMNI is thus redundant, regardless the task and the configuration of its wheels.

Distribution of driving forces through optimization under constraints is the underdetermined system of equations:

- the motor couples  $\tau$  must be inferior to the couple crest of actuators.
- the forces transmitted by the wheels must be inferior to the forces of sliding.
- the solution must lead to the extremum of a given cost function  $g(\Gamma)$ .

$$\begin{cases} F_{cart} = J^T \tau \\ \tau_i < \tau_{iMax}, i \in [1,6] \\ f_{tj} < f_{tjMax}, j \in [1,3] \\ Max(g(\tau_1, \tau_2, \dots, \tau_6)), Min(g(\tau_1, \tau_2, \dots, \tau_6)) \end{cases} \quad (13)$$

The cost function  $g(\tau_1, \tau_2, \dots, \tau_6)$  defines secondary task, such as a function expressing the risk of sliding of one or several wheels.

The movements of the robot involve the set of vehicle's actuators

However, while the long displacements in translation, only tensile actuators are solicited. We suggest two methods of forces distribution on the actuators:

- one establishes a choice among the actuators
- the other considers the set of actuators

#### IV. CRITERION OF ALIENATION OF SLIDING SPEEDS

This first criterion establishes a choice of the closest actuators to their sliding limits.

The minimum standard solution is first calculated using the pseudo inverse of  $J^T$  (Jacobean).

Once the couples are such as :

$$\sqrt{\left(\frac{\tau_{\beta i + \tau_{or}}}{e}\right)^2 + \left(\frac{\tau_{\phi}}{r}\right)^2} \geq 0.8 f_{t_{iMax}} \quad (14)$$

The most important couple of the considered wheel is saturated. The necessary forces to get the dynamic screw are carried over the other wheels. The saturation is set to 80% of the slip limit.

This method is approximate to that employed by Lee in [5]. It presents the disadvantage of generating discontinuities (Fig. 7).

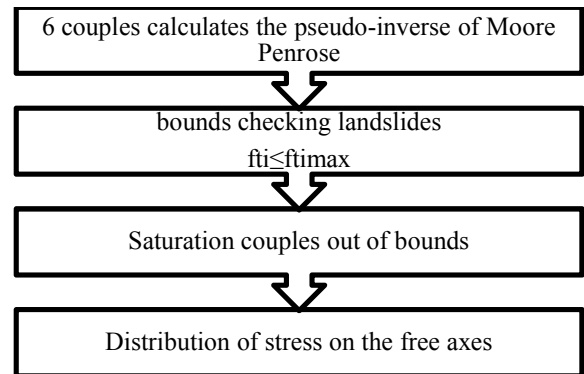


Fig. 7 Algorithm of a distribution function

The previous equations allow calculating the tangential eligible. The maximum tangential force is saturated at 90% of sliding limit, we have:

$$f_{tjMax} = 0,9 \mu N_i \quad (15)$$

$\mu$  is the coefficient of friction and  $N_i$  is the normal charge over the vehicle wheel  $i$ .

The couples resulting a tangential force superior or equal to this threshold, or the couples superior to the maxima couples of actuating, are arbitrary limited.

When the two couples are bounded and when the third wheel arrives on limit, the sliding is unavoidable the separation of couples. The sliding could be avoided only through diminishing the speed and/or the acceleration of the vehicle.

#### V. CRITERION BASED ON THE WEIGHTED SUMS

Contributions actuators traction and steering of the vehicle are obtained by:

$$\begin{pmatrix} F_{\beta} \\ F_{\phi} \end{pmatrix} = \begin{pmatrix} J_{\beta}^T & 0_{3 \times 3} \\ 0_{3 \times 3} & J_{\phi}^T \end{pmatrix} \cdot \tau \quad (16)$$

$$F_{cart} = F_{\beta} + F_{\varphi} \quad (17)$$

Here we present a distribution based on the use of the general solution of a systèmesous-determined [10]:

$$\tau = J^{T+} F_{cart} + ((I - J^{T+} J^T)) \varepsilon \quad (18)$$

$\varepsilon$  is the vector of  $\mathbb{R}^6$ .

The vector  $\varepsilon$  is given by the linear combination:

$$\varepsilon = |F_{\varphi}| \varepsilon_{\varphi} + |F_{\beta}| \varepsilon_{\beta},$$

where  $\varepsilon_{\varphi}$  weights the pairs of traction and  $\varepsilon_{\beta}$  weights couples direction. This approach emphasizes the importance of the choice of axes traction management or those following their involvement in the movement of the platform.

The components of the vector maximum torques traction:

$$\tau_{M\varphi} = (\tau_{M\varphi 1}, \tau_{M\varphi 2}, \tau_{M\varphi 3})^T \quad (19)$$

are imposed either by the maximum torque actuation  $\tau_{AM\varphi}$  whether by couples threshold limit slip  $\tau_{GM\varphi}$ :

$$\tau_{GM\varphi i} = \tau_i \sqrt{(\mu_i N_i)^2 - ((\tau_{\beta i} + \Gamma_{or})/e_i)^2} \quad (20)$$

$$\tau_{M\varphi i} = \min(\tau_{GM\varphi i}, \tau_{AM\varphi})$$

The vector  $\varepsilon_{\varphi}$  is obtained by calculating the gradient of the following cost function:

$$f(\tau_{\varphi 1}, \tau_{\varphi 2}, \tau_{\varphi 3}, \tau_{\beta 1}, \tau_{\beta 2}, \tau_{\beta 3}) = \sum_{i=1}^3 \frac{\tau_{M\varphi i}}{|\tau_{M\varphi}|} (\tau_{M\varphi i} - \tau_{\varphi i})^2 \quad (21)$$

$$\varepsilon_{\varphi} = \frac{\partial f(\tau)}{\partial \tau_{\varphi}}$$

This function maximizes the "distance" of those couples traction maximum traction.

It is a weighted sum that gives more weight to the more involved actuators.

$\varepsilon_{\beta}$  is obtained by a similar approach:

$$\varepsilon_{\beta} = \frac{\partial g(\tau)}{\partial \tau_{\beta}} \quad (22)$$

The use of a continuous filter allows to obtain a continuous distribution of couples involving both actuators than pulling direction. This solution does not guarantee not to reach the limit of slip on one wheel.

## VI. LOAD SAMPLE

For the movement in « square », we have traced in simulation the evolution of the normal load over the vehicle's wheels. The normal load is used in the friction sample and in the calculation of the laws of distribution of engine couples.

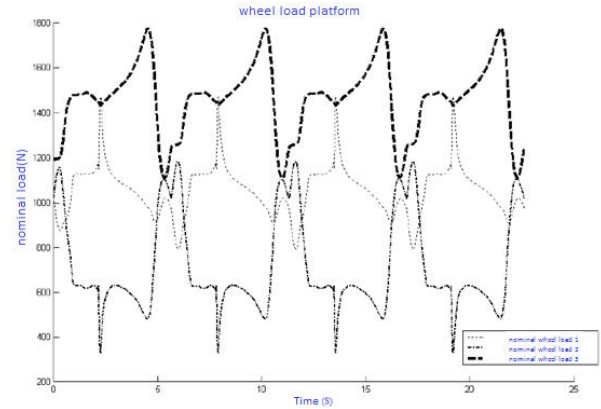


Fig. 8 Normal load during the square movement

Wheel n° 3 of OMNI robot is closer to the center of gravity of the vehicle; it supports a greater average normal load. However, depending on the dynamic effects, each of the three wheels may momentarily become more responsible. The load transfers are important phenomena. For the wheel 2, for example, the normal load range, for the movement of 380N considered to 1150 N.

Variations of the same order can occur on two wheels for other movements.

The calculated load is then used to compensate the friction on the motorized axes and distribute couples actuation.

## VII. SIMULATION RESULTS

In simulation, we compare a simple movement involving actuators only pull effect of the two allocation criteria explained in the theoretical part.

The path (Fig. 9) is a rectilinear movement comprising an acceleration phase with constant speed phase and a deceleration phase. During the two phases dynamics, load transfers between the wheels on the front and one located behind (relative to the direction of displacement) occur.

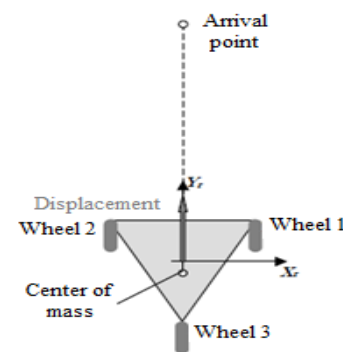


Fig. 9 Configuration of the vehicle

The acceleration is  $2 \text{ m/s}^2$ , speed  $1 \text{ m/s}$ , the displacement is  $90 \text{ cm}$ . Fig. 10 shows the solutions obtained by distributing the drive torque by using the pseudo-inverse of Moore-Penrose criterion No. 1, based on the saturation of the driving torques of the last criterion 2 based on weighted sums.

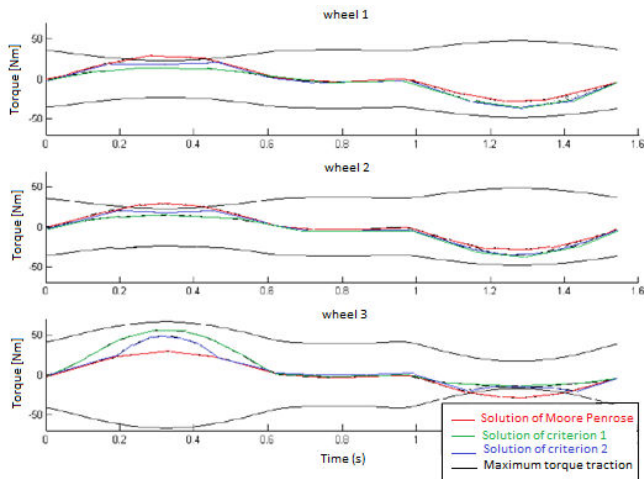


Fig. 10 Couple pulling on three wheels

When the torque setpoints exceed the maximum braking torque, the wheel slip is likely (Fig 10).

Allocation criteria n° 1 and n° 2 prevent landslides obtained using the pseudo-inverse. Couples are simulated at the wheels of the vehicle.

The solution using the pseudo-inverse of Moore Penrose minimizes quadratic efforts, so it gives the best overall energy. This is not the most effective level shifts.

The solution given by the criterion 1 prevents wheel slip remaining close enough to the previous solution. It has the advantage of minimizing operating efforts, as the wheels slip away. It has the disadvantage of establishing a selection between the motorized axes which could cause discontinuities instructions couples.

This solution is unacceptable because it can generate landslides wheel due to switching between motorized axes.

The solution given by the criterion 2 also prevents slippage of the wheel and running on all motorized axes. It has the advantage of being continuous. The "convergence rate" is defined experimentally. Factor leads to a weak solution close to the solution using the pseudo-inverse and factor causes too much overtaking torque setpoints.

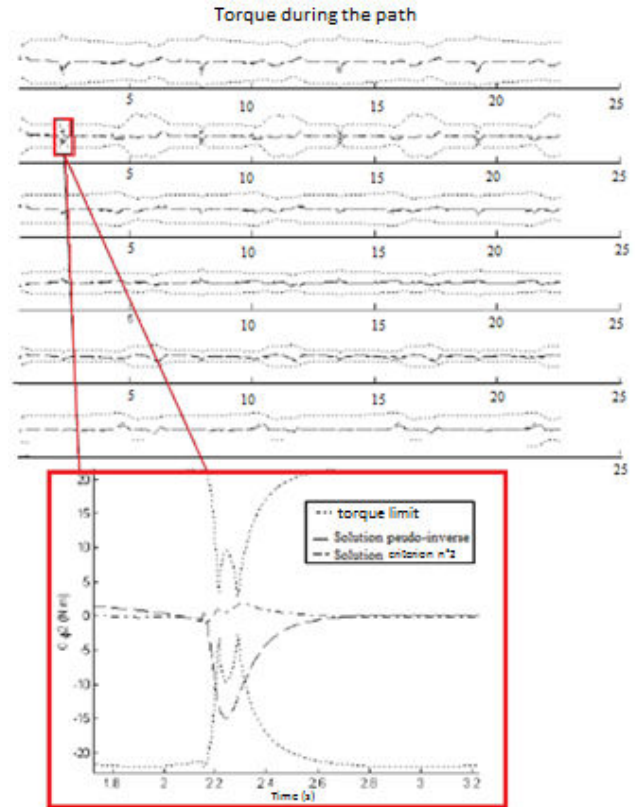


Fig. 11 Couple simulated movement "square"

The simulation was allowed to retain an allocation criterion and evaluate its effectiveness in reducing wheel slippage. It does not, however, quantify the contribution precision associated with the method. This quantification is through experiments on the vehicle.

#### A. Results

The algorithm based on weighted sums, is the only satisfactory from the point of view of continuity. We added a speed loop joint responsibility to compensate for modeling errors, especially those related to the friction model.

The selected control is a predictive control. The movement of the vehicle requires full joint movements. There is only one combination of joint velocities that produces an imposed motion. The vector of actuation speeds is provided by the MCI.

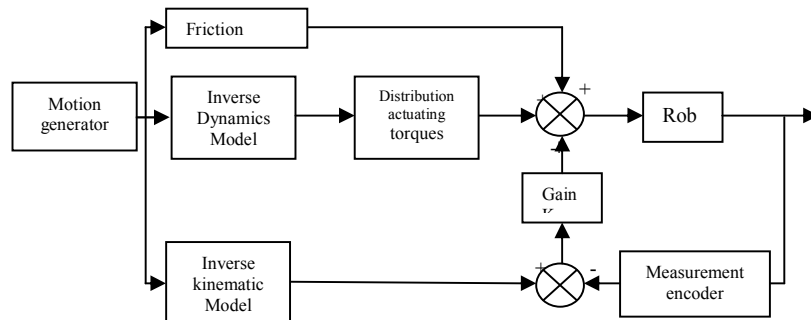


Fig. 12 Dynamic control scheme implemented

This control scheme does not appear explicitly load model; however, it occurs in the calculation of friction and the calculation of the distribution of torque actuation.

The impact of the distribution of engine torque cannot be detected when dynamic phenomena are no longer negligible compared to the friction phenomena. It is therefore necessary to carry out the movements' speeds and accelerations sufficient. Trajectory "square" used. It is performed several times without and then with the optimized distribution of couples actuation.

The effect of the distribution on the accuracy is quantified using the encoder measures. Couples calculated by the conventional method using the pseudo-inverse as well as those give in Fig. 13: Couples engines obtained during the acceleration phase by the method of apportionment based on weighted sums are presented in Fig. 13.

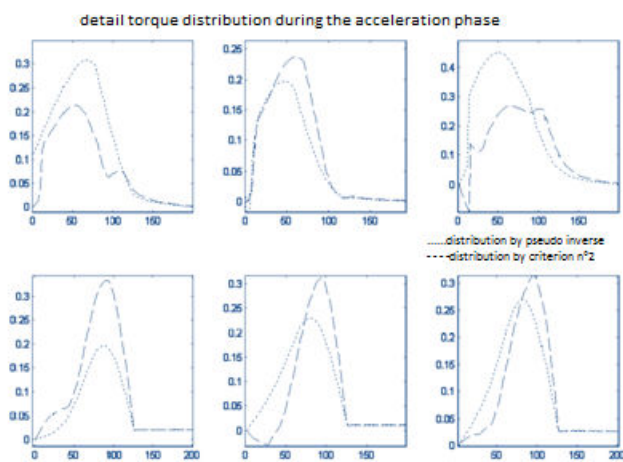


Fig. 13 Torques obtained during the acceleration phase

From successive passages before the four markers, we were able to quantify the contribution of the distribution as well as the repeatability of movement. To accentuate the phenomena of wheel slip, the ground was slippery, thus dropping the coefficient of friction. The trajectory of the vehicle was made without registration by distributing engine torque differently. In the first trial, the allocation method is based on the Pseudo-Inverse Moore-Penrose. In order to avoid errors in the initial positioning of the vehicle, the deviations are measured relative to the first pass in front of each tag. Whatever the method used, the robot drift, away from the beacon at every turn. The distribution function of the normal load on the wheels, however, reduced drift of the vehicle. The trajectory of the robot changes little at every turn.

### VIII. CONCLUSION

The actuation redundancy could be used yet to modify the internal configuration of the robot, like in the case of some robots of swedish wheels where the modification wheels' changes the transmission relations.

This method is simple to implement, however the saturated axes change during the movement, it may generate discontinuities over the couples of engine.

This conduct is incompatible with objectives of continuity of the couples we have fixed.

### REFERENCES

- [1] Julien Aragones Geovany A. Borges and Alain Fournier, *Accuracy improvement for a redundant vehicle*, proceedings of the IEEE International Symposium on Robotics, Stockholm, Sweden, october 2002
- [2] A. Murao, C. Chevallereau, *Trajectoires optimales pour l'amble d'un quadrupède pour des critères énergétiques*, Actes de IEEE Conférence Internationale Francophone d'Automatique, (CIFA), Nantes, France, juillet 2002, pp 528-533
- [3] P. Dauchez, P. Coiffet and A. Fournier, *Cooperation of tow robots in assembly tasks*, Computing techniques for robots, Kogan Page, 1985, pp 197-218
- [4] G. Campion, R. Hossa, *Adaptive output linearizing control of wheeled mobile robot*, proceedings of IFAC symposium on robot control, Nantes, France, September 1997, pp 261-266
- [5] S.H. Lee, B.-J. Yi, S.H. Kim and Y.K. Kwak, *Control of impact disturbance by redundantly actuated mechanism*, proceedings of the IEEE International Conference on Robotics and Automation, Seoul, Korea, may 2001, pp 3734-3741
- [6] Byung-ju Yi and Whee Kuk Kim, *The kinematics for redundantly actuated omni-directional mobile robots*, proceedings of the IEEE International Conference on Robotics and Automation (ICRA), San Francisco, CA, april 2000, pp 2485-2492
- [7] B. Bayle, J.-Y. Fourquet and M. Renaud, *Manipulability analysis for mobile manipulators*, proceedings of the IEEE International Conference on Robotics and Automation, (ICRA), Seoul, Korea, May 2001, pp 1251-1256
- [8] W. Khalil et E. Dombre, *Modélisation identification et commande des robots*, 2<sup>ème</sup> édition revue et augmentée, collection robotique, Hermes 1999
- [9] Vijay Kumar and John, F. Gardner, *Kinematics of redundantly actuated closed chains*, IEEE Transactions on Robotics and Automation, Vol.6, No 2, April 1990, pp 269-274
- [10] D. Folio and V. Cadenat, "A redundancy-based scheme to perform safevision-based tasks amidst obstacles", IEEE Int. Conf. on Robotics and Biomimetics, 2006.
- [11] J. Minguez, F. Lamiroux and J. P. Laumond, "Motion planning and obstacle avoidance", in Springer Handbook of Robotics, B. Siciliano, O. Khatib (Eds.), Springer, 2008, pp. 827-852.